Open Access

Iraqi Journal of Industrial Research (IJOIR)

Journal homepage: http://ijoir.gov.iq

Screw Hole Fatigue in Aluminum Composite Panels: Safe Wind Speed Thresholds Using Hybrid Analysis

Akeel Z. Mahdi*, Orhan S. Abdullah

College of Mechanical Engineering, University of Technology, Iraq

Article information

Article history:
Received: August, 01, 2025
Accepted: September, 30, 2025
Available online: December, 14, 2025

Keywords:
Wind pressure,
Wind loading,
Aluminum composite panel,
Numerical simulation,
Fatigue life

Corresponding Author:
Akeel Z. Mahdi
akeel.z.mahdi@uotechnology.edu.iq

DOI:
https://doi.org/10.53523/ijoirVol12I2ID589

Abstract

Aluminum composite panels (ACPs) are extensively utilized in building facades, but need drilled holes for screw fixation, exposing them susceptible to environmental stresses. This study examines the impact of wind speeds (8–18.72 m/s) on the fatigue life of ACPs. Tensile and fatigue tests were performed on pristine specimens and panels featuring holes of 2, 3, and 4 mm in diameter. The experimental results indicated a significant decrease in fatigue endurance limits (after 10^6 cycles), from 2.3 MPa for the unaltered specimen to 1.45 MPa, 1.424 MPa, and 1.37 MPa for the specimens with 2, 3, and 4 mm holes, respectively. ANSYS Workbench simulations analyzed a 1 m^2 ACP subjected to wind pressure to identify fatigue safety factors. This research determined the safe wind speed thresholds (with a safety factor of 1.25) as 14.41 m/s (pristine), 11.20 m/s (2 mm), 11.12 m/s (3 mm), and 10.79 m/s (4 mm). Results from experiments indicated fatigue limits of 2.3 MPa (pristine), 1.45 MPa (2 mm), 1.424 MPa (3 mm), and 1.37 MPa (4 mm). The pristine specimen exhibited superior fatigue resistance due to the absence of stress concentrations. Dynamic study indicated safe wind speeds of 14.41 m/s (pristine), 11.2 m/s (2 mm), 11.12 m/s (3 mm), and 10.79 m/s (4 mm). Hole diameter directly reduces fatigue performance and allows wind loads. The existence of a 4 mm aperture diminished the fatigue endurance limit by roughly 40% and the safe wind speed threshold by 25% in comparison to the unblemished panel.

1. Introduction

Aluminum composite panels (ACPs) are widely utilized in building facades; nonetheless, they necessitate drilled holes for screw attachment, rendering them susceptible to environmental pressures such as wind loads. Wind loads generate cyclic stresses that significantly affect facade materials [1, 2]. The susceptibility of building envelopes to wind-induced failure, especially at connection points, is a well-documented issue, as demonstrated by recent wind tunnel experiments on metal roofing systems [3]. The analysis of wind data from Iraq, as published by Azhaar et al. [4], based on measurements from 11 meteorological stations at a standard height of 10 meters, indicates that wind speeds are notably higher in the southern portions of the country. This phenomena is due to the largely flat landscape of the region, with the cities of Basra and Nasiriya recording the highest wind speeds, a trend that is particularly evident during the summer months. The performance of ACP, like all composites, is determined by the characteristics of their components [5, 6]. Meticulous selection of these components endows composites with elevated strength, rigidity, favorable fatigue characteristics, reduced weight, and corrosion resistance crucial

qualities for withstanding wind-induced cyclic loads. Fatigue stress refers to the cumulative deterioration resulting from cyclic loading that remains beneath a material's ultimate strength. This is a crucial failure mechanism in engineering structures exposed to wind or vibrations, frequently resulting in catastrophic failure without prior indication, hence necessitating predictive analysis [7]. Investigations looking into the determinants of composite fatigue have examined elements such as surface modifications, connection modelling, and reinforcement influences, consistently indicating that strategic reinforcement can improve impact and fatigue strength [8, 9, and 10]. These findings are very relevant for wind-loaded ACPs where fatigue resistance is critical. Recent research on compromised metal roofing systems has indicated a significant decline in wind resistance and fatigue lifespan attributable to initial seam gaps [11]. Research on composite structures encompasses [12] study on sandwich composites that integrate carbon fiber, aluminum honeycomb, and polymeric matrix, highlighting the distinct mechanical advantages of honeycomb versus foam cores. Ref. [13] presented an exhaustive overview of ACP manufacture and its uses. Current research increasingly focuses on evaluating the mechanical performance of Aluminum Composite Panels (ACPs) under diverse stress conditions. The selective application of reinforcement, such as glass fibres, has been demonstrated to markedly improve the impact resistance and energy absorption of composite panels [14, 15] examined the fatigue properties of Aluminum Foam Sandwich compositions created via different methods. The continued significance of comprehending sandwich structure behavior at severe environments is underscored by recent studies on their cryogenic mechanical performance and failure mechanisms. [16, 17] forecasted the fatigued layers utilizing particular failure measures. Ref. [18] utilized finite element analysis and the Remaining Stress Energy Method (RSE) to investigate fatigue in Composite Pressure Vessels (CPVs). Ref. [19] investigated endurance thresholds and self-heating deterioration in polymer composites subjected to reverse bending [20] assessed fatigue life in laminated composites, whereas [21] examined fatigue life estimation in composite rings employing advanced degradation models. Recently, Ref. [22] examined the fatigue life of ACP under fluctuating wind speeds, indicating its appropriateness for Baghdad's exteriors, provided speeds do not exceed 11 m/s. Research on threaded fasteners subjected to impact fatigue indicates that failure begins at stress concentrators, such as thread roots, resulting in progressive deterioration [23].

Although previous studies have explored different aspects of ACP fatigue, a significant gap remains: the thorough quantitative assessment of the influence of drilled screw holes—a vital practical requirement—on ACP fatigue longevity under genuine wind loading conditions defined by the American standard formula (ASCE 7-16). This study seeks to address this gap through an extensive experimental and numerical analysis of the impact of drilled hole diameters (2, 3, and 4 mm) on the fatigue life of ACPs, establishing definitive safe wind speed thresholds pertinent to Iraqi conditions and offering practical design recommendations.

2. Materials and Methods

2.1. Characteristics of the Sample under Testing (Tensile Test)

The assessment of mechanical properties utilized a commercial 4 mm-thick aluminum composite panel (ACP), serving as a cohesive material system. This structure consisted of Twin 0.1 millimeters of aluminum exterior skins bonded to a polyethylene of 3.8 mm as a core. Tensile characterization conformed to the ASTM E8M-00b standard [24], commended for its proven effectiveness in assessing the mechanical characteristics of aluminum-faced composite materials. This testing methodology assesses the overall mechanical response of the ACP assembly, with the tensile characteristics primarily influenced by the 0.1 mm aluminum layers due to their markedly superior stiffness compared to the core polymer. Test adhered to defined standards utilizing a H50KT- Tinius Olsen universal testing machine for three samples obtained from commercialized ACP sheeting. Testing was conducted in the laboratories of the College of Mechanical Engineering at the University of Technology.

2.2. Methodologies for Experimentation (Fatigue Testing)

The cyclic wind stress encountered was replicate by ACPs on building facades, fatigue testing utilized an HSM20 alternating bending fatigue machine, as illustrated in Figure (1). This technology simulates wind-induced flexural stresses in cladding panels. Specimens underwent regulated alternate bending stress amplitudes beneath the material's yield stress to avert plastic deformation, resulting in S-N curves. The HSM20 machine utilizes material elasticity to transform regulated displacements into applied stresses. Testing persisted until specimen failure or the achievement of the 1-million-cycle endurance threshold, with cycle counts documented by the integrated counter.

The S-N curve, also known as the Whole curve, is an essential instrument in fatigue study that graphs the intensity of cyclic stress (S) against the logarithmic number of cycles to failure (N) for a certain material or component.

Four configurations were examined: pristine specimens (Figure 2) and specimens including holes with diameters of 2 mm, 3 mm, and 4 mm. Experimental S-N curves exhibited hole impacts, but the analytical simulation (ANSYS) simply examined intact panels for reference wind-induced pressures. Factor of Safety margins were established by contrasting the experimental fatigue limitations of perforated specimens with stresses obtained from finite element analysis of the pristine benchmark sample.

Aluminum composite panels (ACPs) are fastened to building facades with screws, requiring drilled holes that create stress concentrations, an essential consideration in fatigue research. To simulate in-service situations with cyclic wind loads on facade-mounted ACPs, hole widths of 2, 3, and 4 mm were used to illustrate a range of stress concentration scenarios. The dimensions directly affect fatigue performance, as larger holes create more stress concentrations and diminish fatigue life. Pristine specimens established a benchmark for separating the impacts of hole-induced stress. Each panel of the holed specimens (2, 3, and 4 mm) featured four holes, one at each corner, to precisely simulate a normal screw-fastened installation. Tensile testing was conducted to determine the mechanical properties of the ACP specimens (Figure 3) utilizing a Tinius Olsen H50KT device. Holes were strategically placed 15 mm from the panel edges, aligning with conventional screw placements, to guarantee that stress concentrations developed at authentic fastening positions where failure begins. A consistent center-to-center spacing of 24.25 cm was upheld along all four corners by industry attachment standards, as in Figure (4).

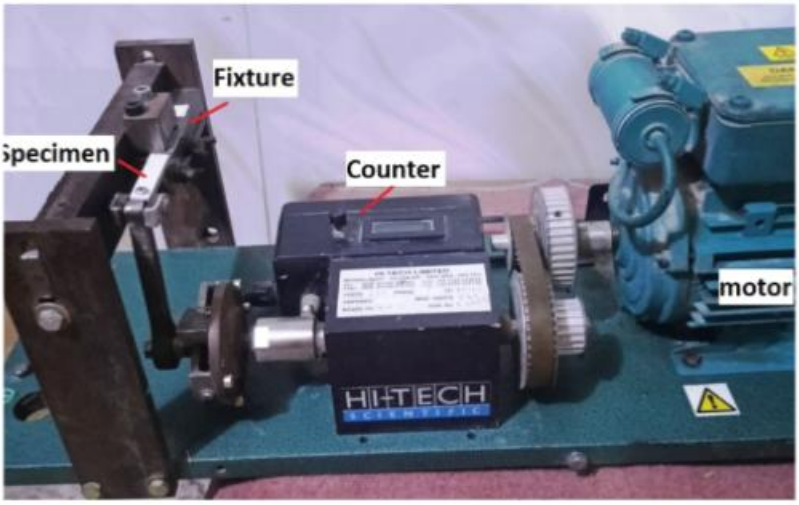

Figure (1): Alternating bending fatigue test (HSM20) apparatus.

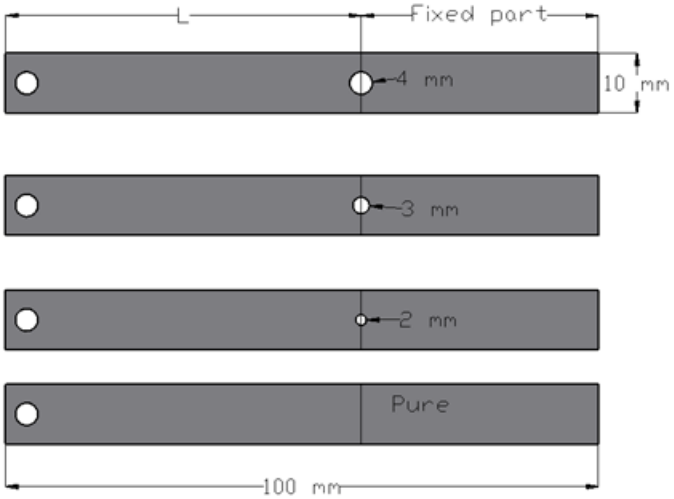

Figure (2): Samples of alternating bending fatigue testing.

Figure (3): The Tinius Olsen H50KT tensile test apparatus.

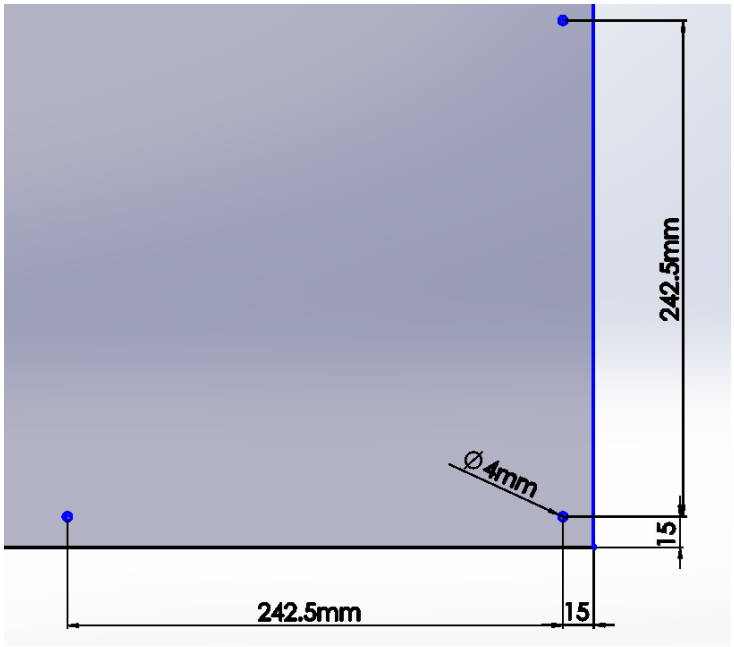

Figure (4): The distance of the hole from the edge.

2.3. Wind Velocity Metrics

Wind speed data were sourced via the Agricultural Meteorological Centre of Iraq's Ministry of Agriculture is located at Al Rashidiya Station in Baghdad, with coordinates N 33.50°, E 44.34° [25]. The analysis covered a five-year dataset from August 1, 2018, to December 1, 2023, indicating a peak wind speed of (18.72 m/s) in Baghdad. Analysis of wind speed data from Baghdad's Al Rashidiya Station (Agricultural Meteorological Centre) for the period 2018–2023 indicated a maximum recorded velocity of 18.72 m/s (Figure 5). Wind effect as pressures has been calculated utilizing the ASCE 7-16 standardized equation $P=0.613V^2$ [26], which represents peak pressure fluctuations during severe wind occurrences. Maximum pressures were utilized in fatigue evaluation as opposed to diminished service-level values (such as 0.6P) due to three considerations: (1) The 0.1 mm aluminum skins demonstrate metal-like fatigue behavior, wherein peak stresses primarily influence Damaged progression; (2) Baghdad's prevailing winds frequently attain between 85 and 90 percent of their nominal velocities [4]; & (3) Safety margins have been established through comparative study of samples tested under similar load conditions.

Velocities ranging from 8 to 18 m/s, in 1 m/s increments, alongside the maximum recorded value of 18.72 meter per second, were assessed for examining cyclic pressure effects across all four ACP versions.

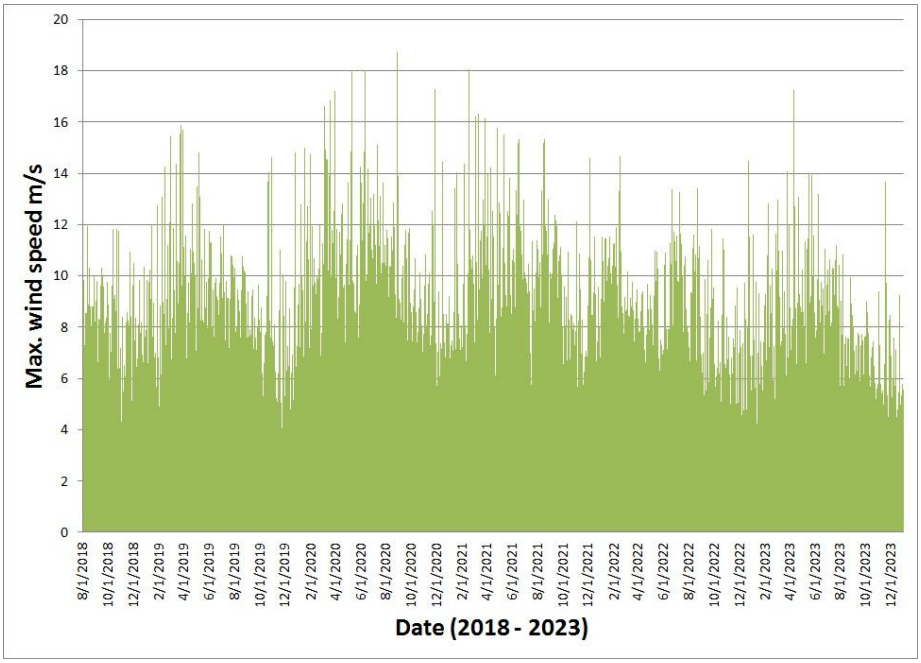

Figure (5): Information regarding the maximum wind velocities from 2018 to 2023.

2.4. Theoretical Framework

This study's analytical framework relies on fundamental engineering ideas and standards. The wind-induced pressure load on the facade was determined using the American Society of Civil Engineers (ASCE) standard formula [26]: $P=0.613 \cdot V^2$, where P represents the wind pressure in Pascals (Pa) and V denotes the wind speed in meters per second (m/s).

In the assessment of fatigue life, the safety factor (SF) was calculated as the ratio of the experimental endurance limit to the maximum stress caused by wind load: $SF=\sigma_{endurance}/\sigma_{max}$ [7].

The stress condition within the ACP was assessed utilizing the Von Mises yield criterion, which is pertinent for forecasting yield initiation in ductile materials such as aluminium. The analogous Von Mises stress (σ) is derived from the primary stresses (σ_1, σ_2, σ_3) as follows:

$$\boldsymbol{\sigma_v} = \sqrt{\frac{(\boldsymbol{\sigma_1} - \boldsymbol{\sigma_1})^2 + (\boldsymbol{\sigma_2} - \boldsymbol{\sigma_3})^2 + (\boldsymbol{\sigma_3} - \boldsymbol{\sigma_1})^2}{\mathbf{2}}}$$

The Peak Von Mises stress was utilized to pinpoint crucial areas susceptible to fatigue fracture initiation [7].

3. Computational Modeling

Safety concerning cycling fatigue as established using finite element modeling of one m² ACP panel using ANSYS Workbench (v17). ACP has been represented as a thin sheet utilizing layered shell181 elements. The boundary conditions were implemented to model a panel securely affixed to a building's substructure. All four edges of the 1 m² panel were designated with defined support conditions, so constraining all degrees of freedom, including translations and rotations. The wind load was delivered as a uniform static pressure perpendicular to the panel's outside surface, as determined by the ASCE 7-16 equation $P=0.613V^2$ [26]. The material properties, encompassing S-N curves for all four specimen configurations (pristine and with 2, 3, and 4 mm holes), were integrated into the secured model. The mesh comprised 28196 hexahedral elements and 57047 nodes (Figure 6), with localized refinement applied around holes to address stress gradients. Wind-generated pressure loading was applied to the

ACP model, as illustrated in Figure (7). The mesh convergence at speed 10m/s, and d= 2mm are illustrated in Figure (8).

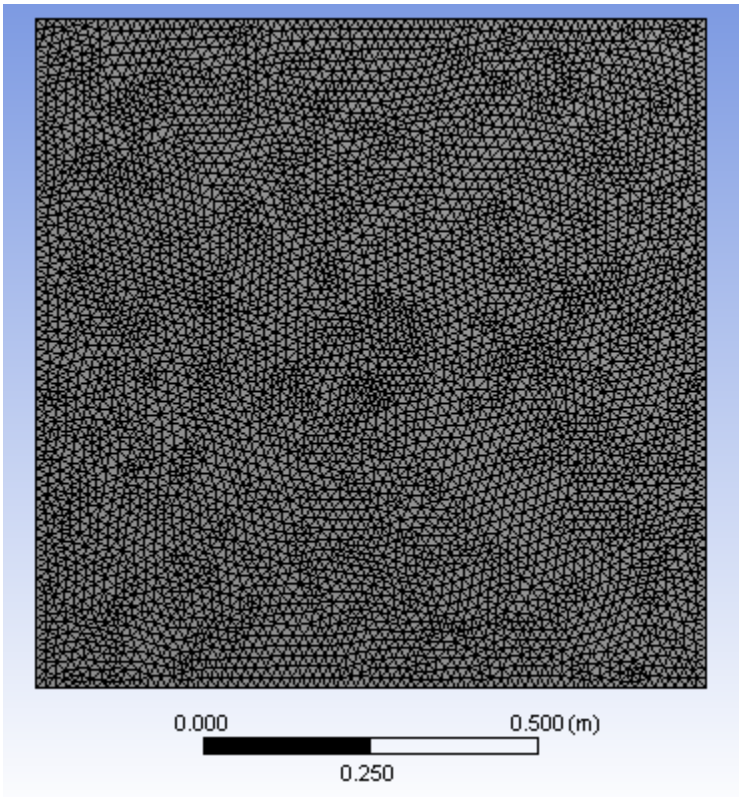

Figure (6): Mesh model of ACP.

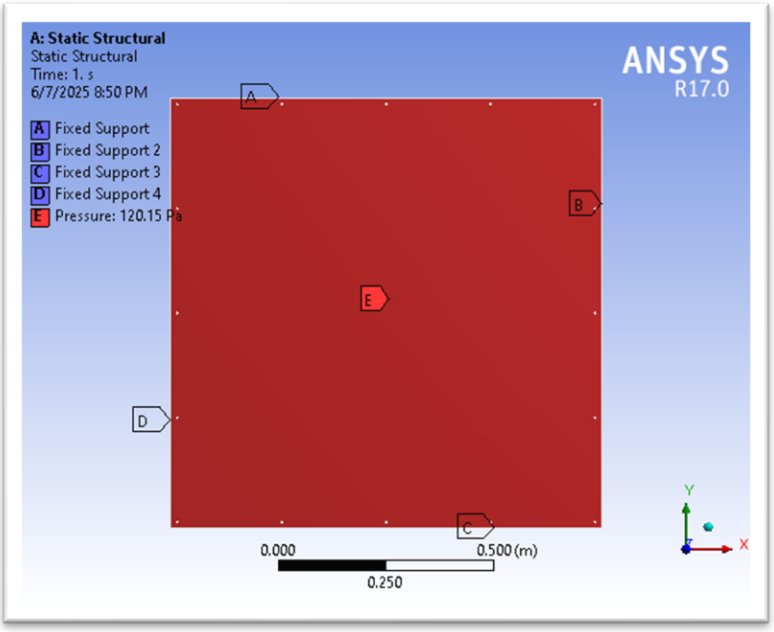

Figure (7): The boundary conditions applied to the ACP Model as a pressure; the support is fixed.

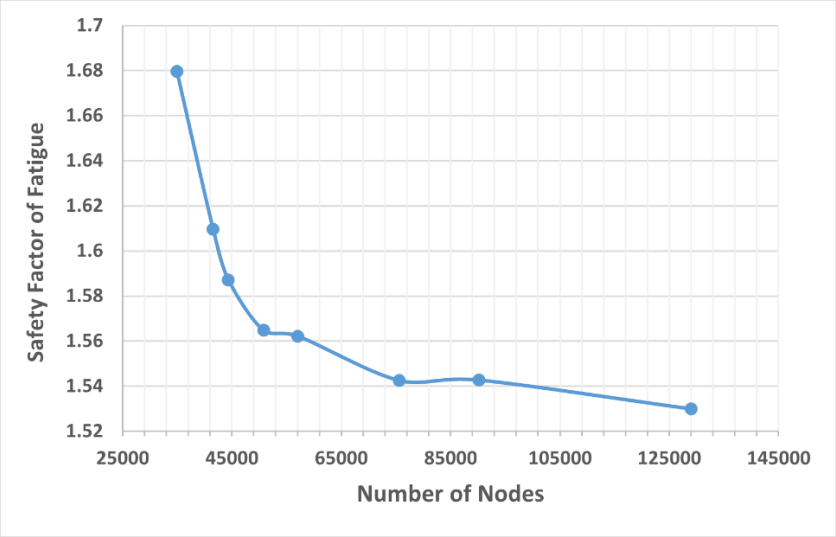

Figure (8): The mesh convergence at speed 10m/s, and d= 2mm.

4. Results and Discussion

Tensile testing of triplicate identical ACP samples determined essential mechanical properties. The experimentally obtained average Young's modulus (363.9 MPa), yield stress (17.26 MPa), and ultimate tensile stress (28.13 MPa) were utilized as parameters for further ANSYS Workbench simulations.

Figure (9) presents experimentally calculated S-N curves for all four configurations: pristine and those with 2, 3, and 4 mm holes. The S-N curves were produced by applying alternate bending stresses beneath the yield point, with cycles to failure recorded at each stress level. In accordance with established protocols [17, 19], the endurance limits (10^6 cycles) were ascertained to be 2.3 MPa (pristine), 1.45 MPa (2 mm), 1.424 MPa (3 mm), and 1.37 MPa (4 mm). The notable decrease in fatigue endurance corresponds with the core tenet of fatigue failure, wherein stress concentrators, such as drilled holes, significantly expedite the progression of localized damage under cyclic loading [7]. The noted decline in fatigue strength with larger hole diameters illustrates the stress concentration phenomenon, wherein geometric irregularities intensify localized strains. The same results for holed specimens suggest that the existence of any hole is more significant than its precise dimension within this range, underscoring the necessity of reducing stress concentrators in facade design under cyclic loading.

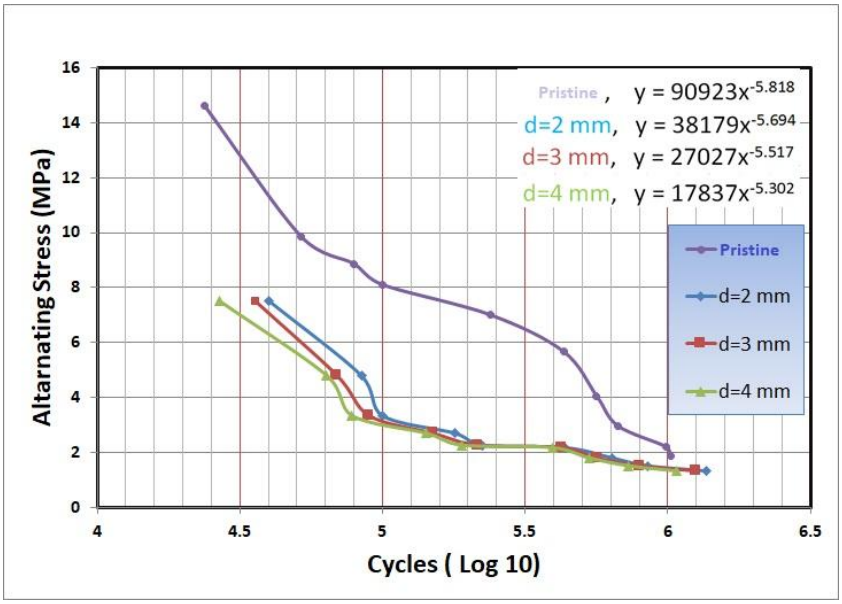

Figure (9): The S-N curve for each situation, illustrating alternating stress against the number of cycles.

Table (1): Safety factor results for all instances owing to fatigue pressure load and wind speed effects.

No.	Wind speed (m/s)	Pressure (Pa)	Safety factor as a result of fatigue load			
			d= 2 mm	d=3 mm	d= 4 mm	pristine
1	8	39.23	2.90	2.83	2.66	4.04
2	9	49.65	2.29	2.23	2.11	3.19
3	10	61.30	1.86	1.81	1.71	2.59
4	11	74.17	1.53	1.49	1.41	2.14
5	12	88.27	1.29	1.26	1.18	1.80
6	13	103.60	1.10	1.07	1.01	1.53
7	14	120.15	0.95	0.92	0.87	1.32
8	15	137.93	0.82	0.80	0.76	1.15
9	16	156.93	0.73	0.71	0.67	1.01
10	17	177.16	0.64	0.63	0.59	0.89
11	18	198.61	0.57	0.56	0.53	0.80
12	18.72	214.82	0.53	0.52	0.49	0.74

Wind-induced alternating fatigue loads were exerted as pressure implemented in the 1 m² ACP variant. The pressure values associated with wind gusts of 8–18.72 m/s have been obtained utilizing the standard ASCE equation $P=0.613V^2$**.** Figure (10) illustrating the inherent power-law correlation between wind velocity and dynamic pressure.

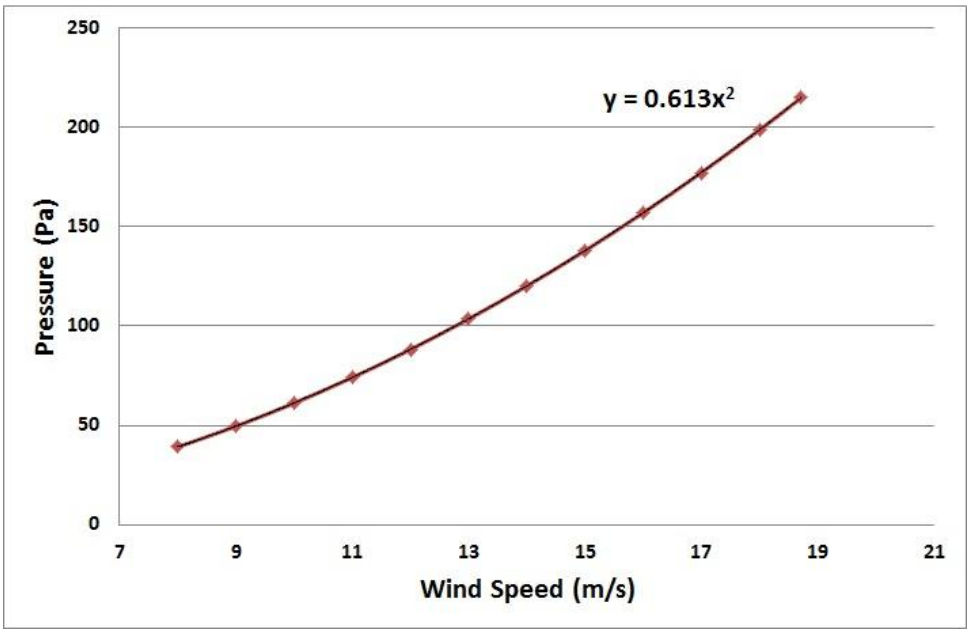

Figure (10): Relationship Both Wind Velocity and Pressure as Defined by the American Standard Formula.

Fatigue safety factors (SF) were calculated using numerical simulation in ANSYS Workbench. The 4 mm-thick, 1 m² ACP model with completely restricted edges was exposed to the calculated pressure loads, as listed in Table (1). Analyses were performed for all four configurations (pristine and 2, 3, 4 mm holes), preserving uniform static mechanical characteristics (Young's modulus = 363.9 MPa, yield stress = 17.26 MPa) while integrating case-specific S-N data. The resultant safety factors are illustrated in Figure (11). The safety factors illustrated in Table

(1) and Figure (11) exhibit a steady decline as wind speed and hole diameter increase. This tendency directly results from the decrease in the experimental endurance limit, as the maximum simulated stress for a specific wind speed remains comparatively consistent across all perforated configurations. The safety factor, defined as the ratio of the endurance limit to the applied stress, diminishes with larger holes due to the reduction of the endurance limit caused by the stress concentration effect. The findings quantitatively demonstrate that stress concentrators substantially diminish the panel's fatigue resistance by lowering its effective endurance strength, thereby decreasing the safe operating wind speed by as much as 25% for a 4 mm hole in comparison to an unblemished panel.

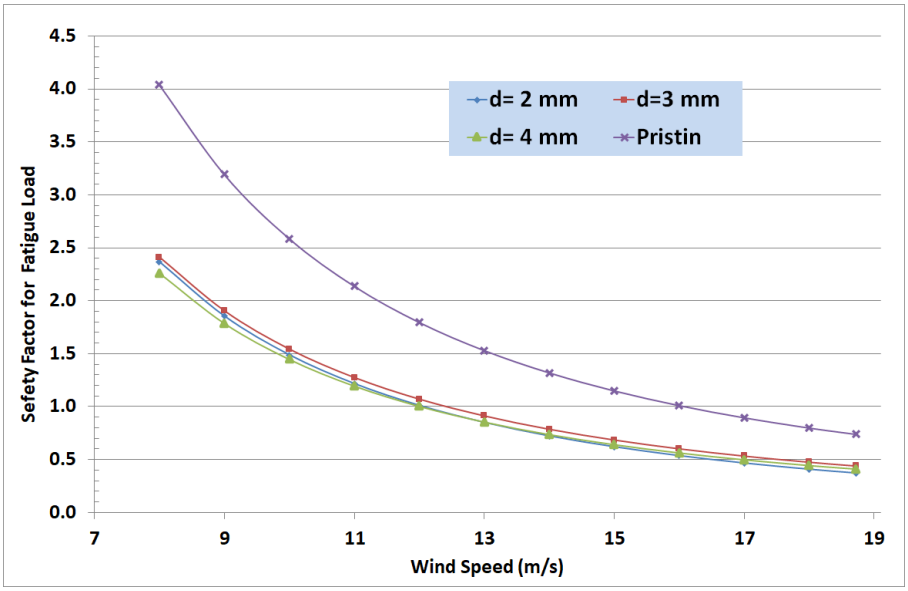

Figure (11): Comparison of fatigue safety factors relative to wind speed across all specimen configurations.

Figure (12) juxtaposes safety factors at varying wind velocities. According to mechanical design guidelines [7], a safety factor (SF) of at least 1.25 establishes the safe operational limit. Thus, the safe wind speeds for the 1 m² panel are: 14.41 m/s (pristine), 11.20 m/s (2 mm), 11.12 m/s (3 mm), and 10.79 m/s (4 mm). This gradual decrease with larger hole diameters (dd) illustrates stress concentration effects, measured by {SF = Fatigue Limit (Experimental) / Maximum Simulated Stress}.

Figures (13 & 14) illustrate the distributions of equivalent (Von Mises) stress. Figure (13) depicts the relationship between stress magnitudes and wind speed across all scenarios, whereas Figure (14) qualitatively represents stress fields at wind speeds of 11 to 14 m/s. Peak stresses are regularly confined along clamped edges due to the concentration of bending moments, in accordance with limited thin-plate theory.

Figures (13 & 14) illustrate two significant events in the Von Mises stress distributions. The maximum stresses are concentrated at the clamped edges, consistent with the boundary conditions that limit all degrees of freedom, resulting in a zone of elevated bending moments. The regions adjacent to the holes exhibit a pronounced stress gradient. The localization of stress, intensified by increasing hole sizes, constitutes the principal locus for fatigue crack development, elucidating the diminished endurance limits recorded experimentally.

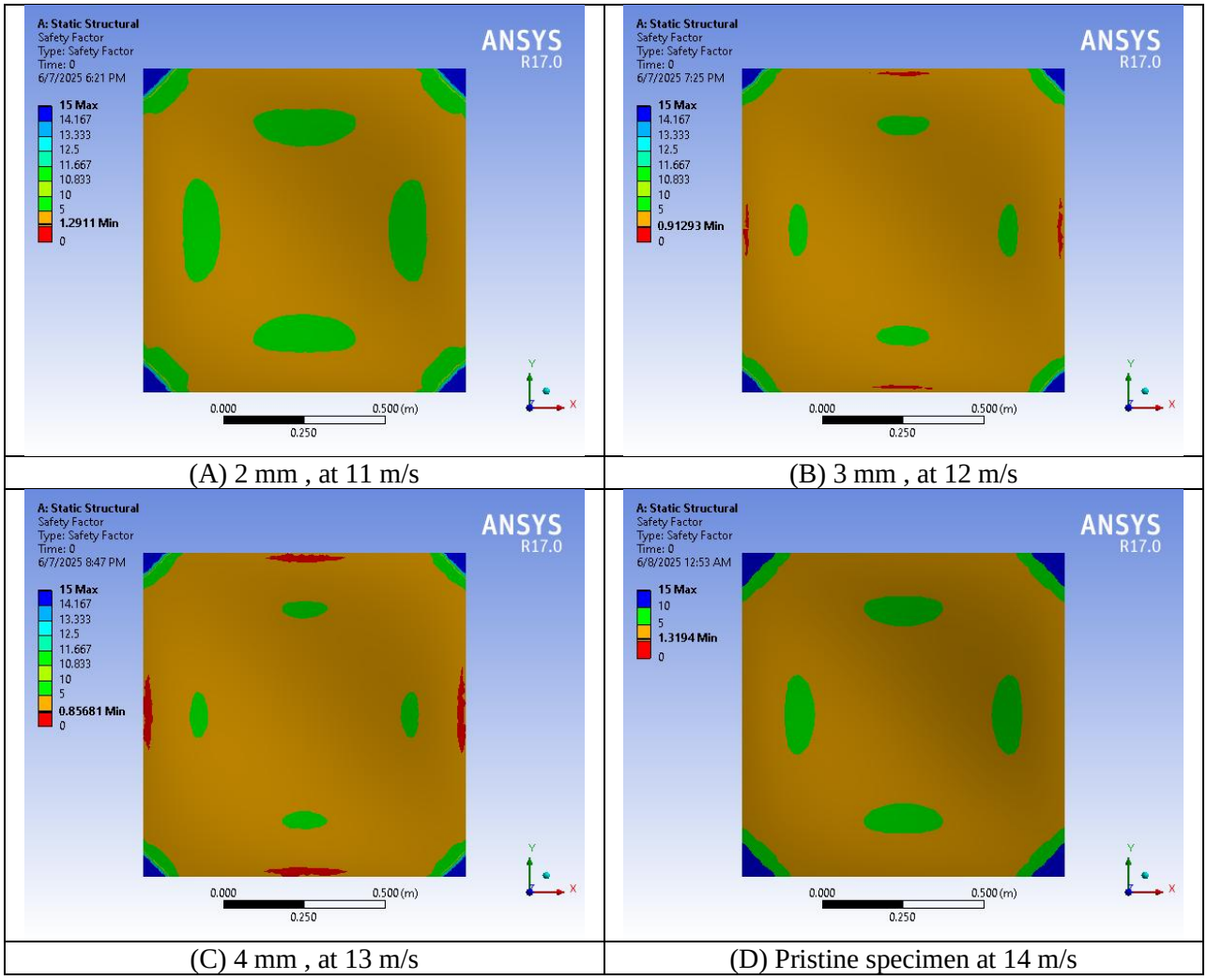

Figure (12): Fatigue safety factor results at key wind velocities.

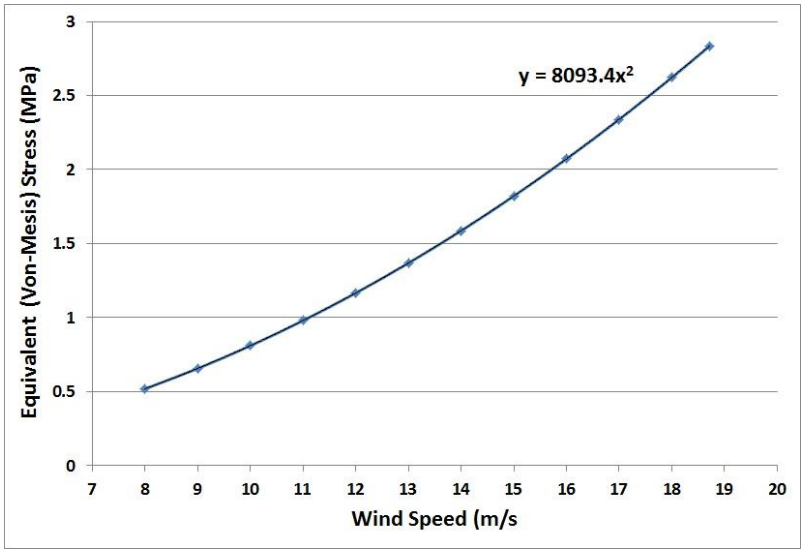

Figure (13): Progression of comparable Von-Mises stress in relation to wind speed throughout all experimental scenarios.

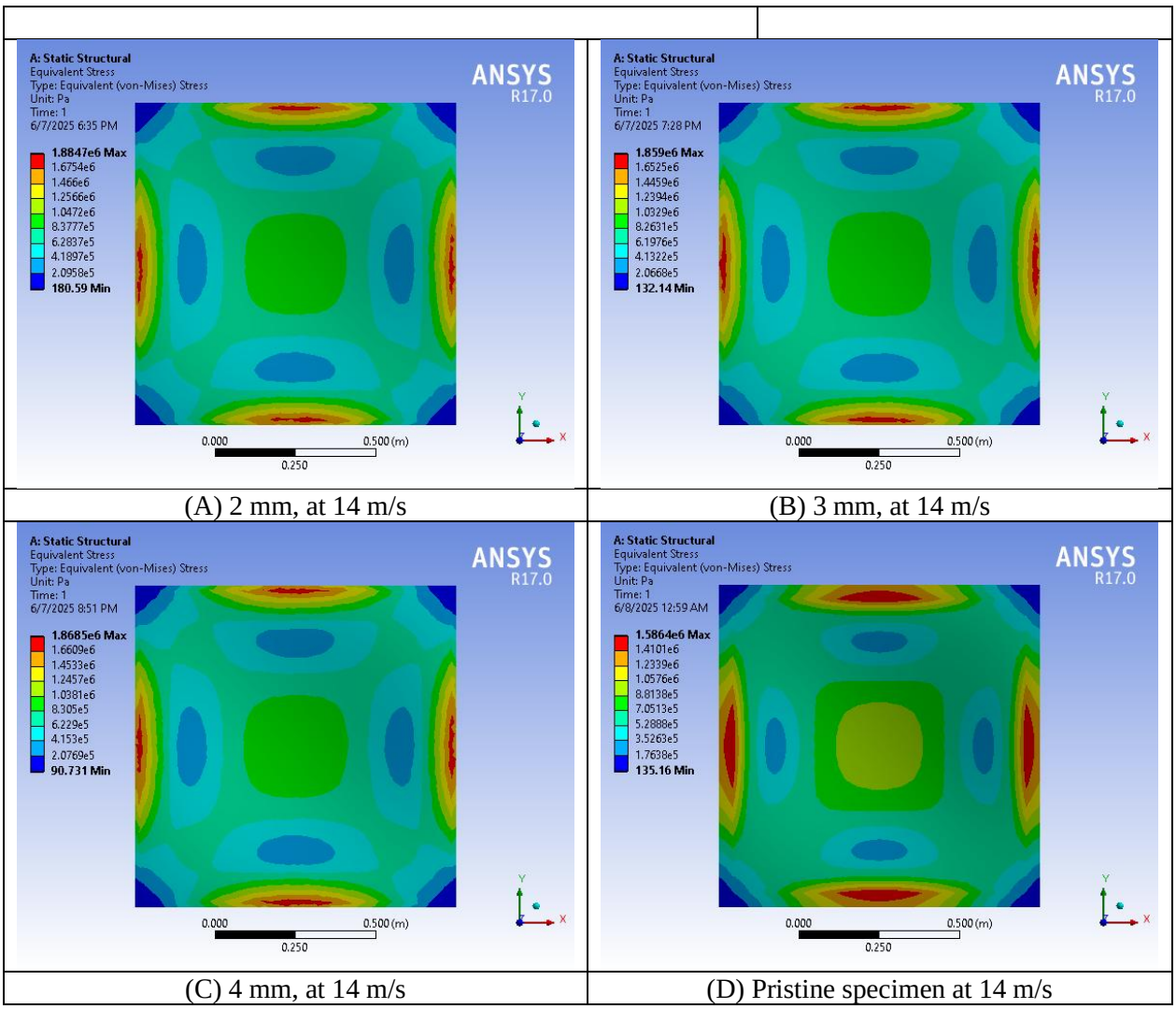

(A) 2 mm, at 14 m/s | (B) 3 mm, at 14 m/s

(C) 4 mm, at 14 m/s | (D) Pristine specimen at 14 m/s

Figure (14): Characteristic Equivalent Von Mises stress distributions.

5. Conclusions

This research delineates essential performance benchmarks for aluminum composite panel (ACP) cladding via an integration of numerical-experimental analysis.

1. The functional wind velocity restrictions over Baghdad city are the following: 14.41 m/s (pristine), 11.20 m/s, 11.12 m/s, and 10.79 m/s for (2, 3, and 4 mm holes), respectively. This 25% drop at 4 mm in comparison to intact the sheets shows the significant influence of stress concentrates upon serviceability.
2. The limitations of endurance of fatigue for one million cycles are: 2.3 MPa for pristine specimens and 1.37–1.45 MPa for holed specimens. The 40.4% reduction at a 4 mm diameter indicates that stress concentrations significantly influence performance during fatigue exceeding fundamental material characteristics.
3. A significant correlation between experimental fatigue lifetimes and numerically calculated safety factors was obtained, confirming the trustworthiness of the hybrid experimental-numerical methodology utilized in this investigation.
4. Von Mises distributions of stress indicate that peak stress concentrates at the clamping borders because of the accumulation of flexing moments. Incremental stress escalation with rising wind velocity. Localized plasticity onset adjacent to hole peripheries under critical loading conditions
5. In practical design, it is advisable to restrict screw hole diameters to under 3 mm in high-wind areas and to contemplate reinforcing panel edges to alleviate stress concentrations resulting from clamping limits.

6. This perimeter-focused arrangement: (i) mitigates mutual stress interference among neighboring fasteners, (ii) maintains structural integrity under cyclic loading, and (iii) precisely emulates edge-constrained high-stress areas where mechanical fasteners convey wind loads to substructures. This arrangement emphasizes experimental faithfulness to actual installation processes, allowing for accurate measurement of hole-size impacts on fatigue behavior for cladding design optimization, in contrast to idealized patterns.

This study formulates a paradigm for evaluating the fatigue resistance of ACPs in wind-exposed areas, emphasizing hole size optimization as a vital design consideration.

Conflict of Interest Declaration: The authors assert the absence of any financial, personal, or professional conflicts of interest that may affect this research or its results.

Acknowledgements
The authors express their gratitude to the Labs of the College of Mech. Eng. - (University of Technology, Baghdad), for offering experiment infrastructure. We express our gratitude to Iraq's Ministry of Agriculture and, Agricultural Meteorological Centre to provide velocity of wind velocity datasets.

References

[1] A. K. Azad, M. M. Alam, and I. M. Rafiqul, "Statistical analysis of wind gust at coastal sites of Bangladesh," *Int. J. Energy Machinery*, vol. 3, 2010, Art. no. 8.
[2] M. Azhaar, N. Sura, A. B. Khamees, and M. A. Abdulsattar, "The temporal and spatial distribution of wind factor in Iraq Karbala," *Int. J. Mod. Sci*., vol. 6, no. 1, 2020, Art. no. 8, doi: 10.33640/2405-609X.1363.
[3] W. B. Han et al., "Wind resistance performance and reinforcement measures of standing seam metal roofs based on wind tunnel tests," *Adv. Steel Constr*., vol. 21, no. 1, pp. 1–20, 2025, doi: 10.18057/IJASC.2025.21.1.1.
[4] A. K. Mishaal, A. M. Abd Ali, and A. B. Khamees, "Wind distribution map of Iraq - A comparative study," *In Proc. 2nd Int. Sci. Conf. Al-Ayen Univ*., 2020, vol. 928, Art. no. 022044, doi: 10.1088/1757-899X/928/2/022044.
[5] O. S. Abdullah and A. Z. Mahdi, "Investigation of thermal fatigue behavior for HDPE composites reinforced by nano alumina," *Mech. Adv. Compos. Struct.*, vol. 11, pp. 335–340, 2024, doi: 10.22075/macs.2024.31577.1553.
[6] A. AIT SAID, K. BEY, and H. MZAD, "Mechanical fatigue test of aluminum composite panel (ACP) with aramid Nida-Core under cyclic bending," *J. Mech. Eng.*, vol. 70, no. 2, pp. 1–10, 2020, doi: 10.2478/scjme-2020-0015.
[7] B. A. Miller, "Fatigue Failures," *in Failure Analysis and Prevention*, vol. 11, ASM Handbook, 2002, p. 1470.
[8] A. Boisseau, P. Davies, and F. Thiebaud, "Fatigue behaviour of glass fibre reinforced composites for ocean energy conversion systems," *Appl. Compos. Mater*., vol. 20, pp. 145–155, 2013, doi: 10.1007/s10443-012-9260-0.
[9] D. S. Kumar, K. N. S. Suman, P. Palash, and C. T. Sasanka, "Performance evaluation of surface modified nano Al2O3 (p) reinforced AZ91E composites under impact and fatigue loading conditions," *J. Mech. Eng*., vol. 70, no. 1, pp. 29–38, 2020, doi: 10.2478/scjme-2020-0003.
[10] A. Dovhopolov et al., "Modeling of a stress-strain state of detachable connection in details of reinforced composite materials with CEA method," *J. Mech. Eng*., vol. 70, no. 1, pp. 17–28, 2020, doi: 10.2478/scjme-2020-0002.
[11] K. Xu, L. Zhi, N. Zhang, K. Zhou, and A. Li, "Wind-resistance performance investigation and fatigue life analysis of impaired standing seam metal roof systems," J. Build. Eng., vol. 111, 2025, Art. no. 113463, doi: 10.1016/j.jobe.2025.113463.
[12] S. Dinesh, T. Rajasekaran, M. Dhanasekaran, and K. Vigneshwaran, "Experimental testing on mechanical properties of sandwich structured carbon fibers reinforced composites," *in Proc. 2nd Int. Conf. Adv. Mech. Eng*., 2018, vol. 402, Art. no. 012180, doi: 10.1088/1757-899X/402/1/012180.
[13] M. Selvakumar, D. J. D. James, and K. R. Thangadurai, "A deep study on aluminum composite panel: applications, merits, and demerits," *Int. J. Mech. Eng*., vol. 6, 2021.

[14] E. Şimşir, "Study of Impact Behavior of Glass-Fiber-Reinforced Aluminum Composite Sandwich Panels at Constant Energy Levels," Coatings, vol. 15, no. 3, 2025, Art. no. 299, doi: 10.3390/coatings15030299.
[15] S. Liu et al., "Fatigue of an aluminum foam sandwich formed by powder metallurgy," *Materials*, vol. 16, no. 3, 2023, Art. no. 1226, doi: 10.3390/ma16031226.
[16] H. Lei et al., "Cryogenic mechanics and failure behaviors of CFRP/aluminum honeycomb sandwich structures," *Compos. Sci. Technol*., p. 111310, 2025, doi: 10.1016/j.compscitech.2025.111310.
[17] S. Zhou and X. Wu, "Fatigue life prediction of composite laminates by fatigue master curves," *J. Mater. Res. Technol*., vol. 8, no. 6, pp. 6094–6105, 2019, doi: 10.1016/j.jmrt.2019.10.003.
[18] A. Kabiri Ataabadi and G. A. Jeyed, "Strength analysis and fatigue life estimation of composite pressure vessel (CPV) based on the residual strain energy (RSE) approach," *Int. J. Comput. Methods Eng. Sci. Mech*., vol. 22, no. 2, pp. 81–102, 2020, doi: 10.1080/15502287.2020.1849446.
[19] A. Katumin and D. Wachla, "Determination of fatigue limit of polymeric composites in fully reversed bending loading mode using self-heating effect," *J. Compos. Mater*., vol. 53, no. 1, pp. 83–91, 2018, doi: 10.1177/0021998318780454.
[20] M. M. Shokrieh and F. Taheri-Behrooz, "Fatigue life prediction of composite materials based on progressive damage modeling," *in Fatigue Life Prediction of Composites and Composite Structures. Darya Ganj: Woodhead Publishing*, 2010, pp. 249–292, doi: 10.1533/9781845699796.2.249.
[21] P. Shabani, F. Taheri-Behrooz, S. Maleki, and M. Hasheminasab, "Life prediction of a notched composite ring using progressive fatigue damage models," *Compos. Part B Eng*., vol. 165, pp. 754–763, 2019, doi: 10.1016/j.compositesb.2019.02.013.
[22] A. Z. Mahdi and O. S. Abdullah, "Experimental and numerical study of fatigue life for Aluminum Composite Panel (ACP) under the ranges of wind speed effect," *Aust. J. Mech. Eng*., pp. 1–9, 2023, doi: 10.1080/14484846.2023.2295108.
[23] C. Zhang et al., "Failure behaviours of steel/aluminium threaded connections under impact fatigue," Eng. Fail. Anal., vol. 174, 2025, Art. no. 109473, doi: 10.1016/j.engfailanal.2025.109473.
[24] *Standard Test Methods for Tension Testing of Metallic Materials [Metric]*, ASTM E8M-00b, ASTM International, 2001.
[25] Iraq Meteorological Organization. *Agromet Iraq*. [Online]. Available: https://www.agromet.gov.iq/index.php
[26] *Minimum Design Loads for Buildings and Other Structures*, ASCE/SEI 7-16, American Society of Civil Engineers, 2017.